



Comparative study on the photoelectrocatalytic inactivation of *Escherichia coli* K-12 and its mutant *Escherichia coli* BW25113 using TiO₂ nanotubes as a photoanode



Xin Nie^{a,d}, Guiying Li^a, Minghui Gao^c, Hongwei Sun^{a,d}, Xiaolu Liu^b, Huijun Zhao^b, Po-Keung Wong^c, Taicheng An^{a,*}

^a State Key Laboratory of Organic Geochemistry, Guangzhou Institute of Geochemistry, Chinese Academy of Sciences, Guangzhou 510640, China

^b Centre for Clean Environment and Energy, Griffith University, Gold Coast Campus, QLD 4222, Australia

^c School of Life Sciences, The Chinese University of Hong Kong, Shatin, NT, Hong Kong Special Administrative Region

^d University of Chinese Academy of Sciences, Beijing 100049, China

ARTICLE INFO

Article history:

Received 27 June 2013

Received in revised form 3 September 2013

Accepted 22 September 2013

Available online 30 September 2013

Keywords:

Photoelectrocatalytic inactivation

E. coli

Mutant strain

Reactive species

Inactivation mechanism

ABSTRACT

Photoelectrocatalytic (PEC) and photocatalytic (PC) inactivation of ancestor *Escherichia coli* K-12 and its mutant *E. coli* BW25113 were systematically compared using a TiO₂ nanotubular photoanode. The results showed that PEC inactivation was more effective to both bacterial strains than PC process, and *E. coli* BW25113 showed higher resistance than *E. coli* K-12 in both PEC and PC systems. The findings indicate that the two strains with different genes are varied in their susceptibilities and responses to the PEC and PC treatments. The h⁺ was found to be the major reactive species and predominantly responsible for PEC inactivation. Scanning electron microscopy images demonstrated that the cells were severely damaged and resulted in a leakage of the intracellular components during PEC inactivation process. For a given bacterial strain, no significant effect was found on the PEC inactivation efficiency as different electrolytes were employed. However, in the presence of NaCl or NaBr, PEC inactivation efficiencies of both strains were remarkably enhanced. This phenomenon can be attributed to the efficient formation of halide and dihalide radical anions during PEC process. The different efficiencies of the two bacterial strains under same conditions can be ascribed to their different abilities to resist the inactivation of bacterial strains with different genotypes.

© 2013 Elsevier B.V. All rights reserved.

1. Introduction

Various microorganisms such as viruses, bacteria, and fungi have currently received considerable attention because of their abundance in natural and wastewaters. These pathogenic microorganisms are extremely harmful and can cause various diseases to animals and human. Pathogens in drinking water and wastewater may pose serious problems on the safety of the water supply. Most of the conventional disinfection methods, such as chlorination, ozonation, and ultraviolet (UV) irradiation, have limitations, although these techniques have been widely used over the past decades [1–3]. These limitations include the production of unintentional toxic by-products [4], energy and labor intensive, and pathogens recalcitrant to some traditional disinfection techniques. Therefore, great effort has recently been exerted to develop new disinfection technologies that are inexpensive, safe, and effective.

The semiconductor photocatalytic (PC) process is considered as a promising alternative technology to traditional disinfection [5–13].

Since Matsunaga et al. [6] first reported their pioneering work on the PC inactivation of microorganisms using UV-irradiated titanium dioxide (TiO₂) powder, extensive studies have been dedicated to PC inactivation of various microorganisms using TiO₂ as photocatalysts [7,9,14–16]. However, the inactivation is limited because of the rapid charge recombination on the surface of powder form TiO₂ that decreases the concentration of reactive species (RSs) and subsequently the microbial inactivation efficiency [7,9,14–16]. This limitation can be surpassed by synthesizing new form of efficient photocatalysts or immobilizing TiO₂ catalysts onto conductors that enables the application of electrochemical techniques. Moreover, a photoelectrocatalytic (PEC) system with an external potential bias can provide a superior solution by suppressing the charge recombination [17–24]. Furthermore, compared to the powder forms of TiO₂, TiO₂ nanotubes can transfer electron more effectively due to their special cannular structure [22,25–27], and subsequently the bactericidal efficiencies in a PEC system can be remarkably enhanced [17,22,23,27].

* Corresponding author. Tel.: +86 20 85291501; fax: +86 20 85290706.

E-mail address: antc99@gig.ac.cn (T. An).

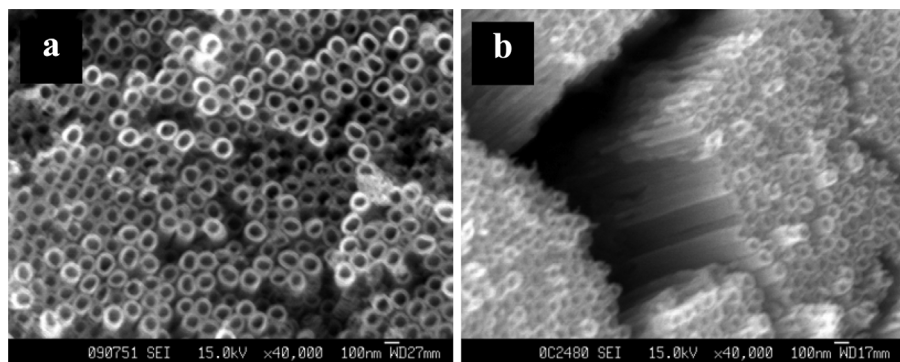


Fig. 1. Top (a) and cross-sectional (b) FESEM images of TiO_2 nanotubular photoanode fabricated in ethylene glycol solution with 0.2 M NH_4F and 0.5 M HAc anodized at 30 V for 24 h.

Under UV ($\lambda < 385$ nm) irradiation, various RSs, such as h^+ , $\cdot\text{OH}$, $\text{O}_2\cdot^-$, and H_2O_2 , etc., could be produced at TiO_2 , which can degrade organic pollutants as well as inactivate bacteria by changing the cell membrane permeability of microbes, resulting in a leakage of cellular components [8,9,14–16,28,29]. However, the half-life of most RSs is very short, and they probably exist only in the region near the catalyst surface because they can be readily quenched in aqueous environment [9]. To date, the contributions of different RSs to bacterial inactivation remain controversial. The majority of recent studies have primarily focused on the PC inactivation efficiency of a single bacterial strain, while comparative studies on PC inactivation of a series of closely related bacterial mutant strains are rarely performed [30]. Nevertheless, to date, a comparative study of PEC inactivation of different mutants using highly ordered TiO_2 nanotubular photoanode has not been attempted yet.

Therefore, to investigate the effect of different genotypes on the susceptibility toward treatment, the PC and PEC inactivation of ancestor strain *Escherichia coli* K-12 and its mutant *E. coli* BW25113 constructed using single-gene deletion of all nonessential genes in *E. coli* K-12, were comparatively conducted in a thin-layer reactor using highly ordered TiO_2 nanotubes as photoanode. In addition, the contribution of the RSs and the morphological changes of two different strains during PEC inactivation process were also clarified by scavenging experiments and field-emission scanning electron microscopy (FESEM), respectively. Furthermore, halide ions (Cl^- and Br^-) were also employed to investigate their enhancement on the inactivation kinetics during PC and PEC processes. Finally, a possible bactericidal mechanism was discussed.

2. Experimental

2.1. Photoanode preparation

Highly oriented TiO_2 nanotube arrays were prepared using potentiostatic anodization in a two-electrode electrochemical cell, as described in our previous study [31]. After optimization, the TiO_2 nanotube with best PC performance was synthesized as follows. A mixture of ethylene glycol, 0.50 M HAc, and 0.20 M NH_4F was used as an electrolyte. Ti foils were pre-anodized for 4 h at 30 V, sonicated in deionized water to remove the fibers, and anodized for another 24 h at 30 V. Finally, the as-synthesized TiO_2 nanotube was washed with deionized water and subsequently annealed at 500 °C for 2 h with a heating and cooling rate of 2 °C min⁻¹. The surface morphologies of the resultant samples were observed using a FESEM (JEOL JSM-6330F). As shown in Fig. 1, the free standing nanotubes with inner diameter of ca. 80 nm and length of 8 μm were obtained for later applications.

2.2. Bacterial cell preparation

E. coli K-12 and its mutant *E. coli* BW25113 (The Coli Genetic Stock Center at Yale University, USA) were selected as model bacterial strains to evaluate the PEC and PC inactivation efficiencies in the absence and presence of NaCl and NaBr. Bacterial strains were cultured in nutrient broth at 37 °C for 16 h with shaking 200 rpm. The cells were successively harvested by centrifugation at 4000 rpm for 15 min, washed twice with sterilized 0.2 M NaNO_3 , and resuspended in 0.2 M NaNO_3 solution to the initial population of 1.10×10^7 colony forming units per milliliter (CFU mL⁻¹).

2.3. Procedures for bacterial inactivation

The PC and PEC inactivation experiments were all performed in a thin-layer photoelectrochemical reactor with 100 μL reaction chamber [5] under constant applied potential of +1.0 V [31] and with a TiO_2 nanotubular photoanode illuminated by a UV-light emitting diode array (NCCU033 (T), Nichia Corporation, Australia, wavelength of 365 nm with a spectrum half width of 8 nm). The light intensity was adjusted using a power supply and controlled at 28 mW cm⁻². For the PEC experiment, a platinum foil and a saturated Ag/AgCl were served as counter and reference electrodes, respectively. PC and light control experiments used as control were conducted under identical experimental conditions as PEC, except the electrochemical system was disconnected and only UV irradiation was used, respectively.

Solution containing bacteria and NaNO_3 was injected into the reactor with a series of constant speeds to adjust disinfection time using a constant-flow pump (HX-901A, Guangzhou Huaxi Medical Technology Co., Ltd., China). Prior to each experiment, the reactor was washed several times to remove the residuals produced from the bacterial decomposition. A sufficient volume of inactivation solution was collected for further analysis of final bacterial survivability by diluting with deionized water and spreading a small amount uniformly onto a nutrient agar plate (three plate repeats per sample). Plates were incubated at 37 °C for 16 h, and bacterial colonies were counted.

2.4. Preparation procedure for bacterial SEM study

The solution with bacteria was collected and centrifuged before and after inactivation. The cells were initially prefixed by 2.5% glutaraldehyde for 4 h, attached on a glass slide, treated with 0.1% polylysine, and subsequently washed with 0.1% phosphate-buffered saline, six times each for 20 min. The specimens were then dehydrated by a graded series of ethanol (30% for 15 min, 50% for 15 min, 70% for 12 h, 90% for 15 min and then 100% for 15 min 3 times) and 100% butyl alcohol three times each for 15 min,

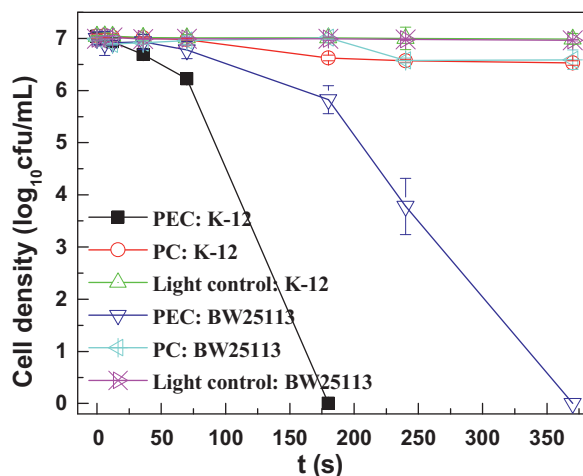


Fig. 2. PC and PEC inactivation of *E. coli* K-12 and *E. coli* BW25113.

respectively. The resultant cells were finally critical point dried, gold sputter coated on the substrates and were visualized using FESEM.

3. Results and discussion

3.1. Comparison of inactivation performances of PEC and PC systems

The PEC and PC inactivation profiles of *E. coli* K-12 and its mutant *E. coli* BW25113 are shown in Fig. 2. The light control experiment showed no significant changes in the cell concentration within 370 s, suggesting that UV light had no toxic effect on bacteria. Comparatively, the inactivation efficiencies within the same investigated reaction times follow the order of PEC > PC for both strains. For *E. coli* K-12, all bacterial cells were completely killed by the PEC process within 180 s, whereas only ca. 0.5-log reduction of bacterial cells was achieved with PC treatment, even with a prolonged of 370 s. In contrast, the mutant *E. coli* BW25113 showed higher resistance to PEC and PC treatments compared with its *E. coli* K-12. Complete PEC inactivation of *E. coli* BW25113 was achieved within 370 s, whereas only ca. 0.4-log reduction of bacterial cells was obtained for PC within the same period. Higher inactivation activity of PEC than PC for both strains could be explained by the following reasons. Firstly, compared with TiO₂ nanoparticle photoanode, higher light adsorption capability and more efficient charge transfer can be obtained with TiO₂ nanotubular photoanode [32]. Moreover, higher surface area of TiO₂ nanotubular photoanode can induce a higher photocurrent [17,31], resulting in rapid inactivation rate. For instance, to completely kill *E. coli* K-12, the PEC inactivation time in this study is ca. 1.7 times faster than that in our previous study under identical experimental conditions, except that the photoanode was immobilized with TiO₂ nanoparticles onto conducting glass in the previous study [33]. Hayden et al. [22] also reported that TiO₂ nanotubes offer distinct advantages over TiO₂ films in inactivating *E. coli* in wastewater. Second, the applied potential bias serves as an external driving force that can timely remove the photogenerated electrons and effectively suppress photoelectrons/photoholes recombination to prolong the lifetime of the photoholes for direct inactivation. Hence, the inactivation efficiency was enhanced significantly [34–37].

3.2. Roles of different reactive species in PEC system

In PEC bacterial inactivation, various RSs, such as h⁺, •OH, O₂^{•-}, and H₂O₂, are produced and may be involved in the bacterial

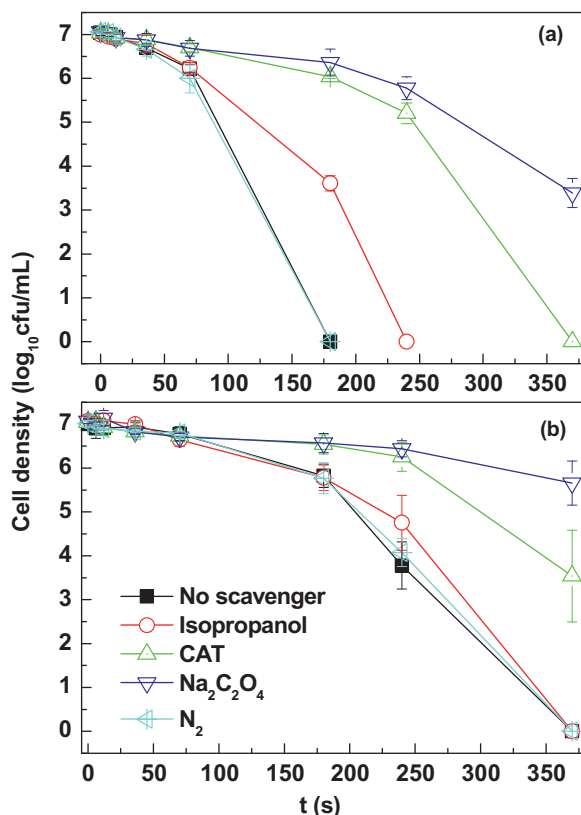


Fig. 3. PEC inactivation of *E. coli* K-12 (a) and *E. coli* BW25113 (b) with different scavengers (1 mmol/L isopropanol, 0.05 μ mol/L CAT, and 1 mmol/L Na₂C₂O₄, N₂).

inactivation [7]. Different scavengers were used to remove RSs to determine the dominant RSs responsible for bacterial inactivation. For instance, 1 mM isopropanol was used to scavenge •OH_{bulk}, 0.05 μ M catalase (CAT) was used to remove H₂O₂, 1 mM Na₂C₂O₄ was used to quench h⁺, and N₂ was used to exclude O₂ to remove O₂^{•-} [13]. The PEC inactivation profiles of *E. coli* K-12 and *E. coli* BW25113 with or without scavengers are shown in Fig. 3. The complete inactivation of *E. coli* K-12 and *E. coli* BW25113 can be achieved within 180 and 370 s, respectively, without the addition of any scavengers. In the presence of 1 mM isopropanol, the inactivation of the two strains slightly decreased, and the complete inactivation of *E. coli* K-12 and *E. coli* BW25113 were achieved at 240 and 370 s, respectively. These phenomena indicate a minor contribution of •OH during the PEC inactivation for both strains. However, an obvious inhibitory effect was observed for both strains when 0.05 μ M CAT was added. The complete inactivation of *E. coli* K-12 and ca. 3.5-log reduction of *E. coli* BW25113 was obtained within 370 s, implying that H₂O₂ plays an important role during this inactivation process. Expectedly, quenching h⁺ by 1 mM Na₂C₂O₄ also resulted in a significant decrease in PEC inactivation efficiency. Only ca. 3.7-log and 1.4-log reductions in cell densities were obtained for *E. coli* K-12 and *E. coli* BW25113 within 370 s, respectively. In contrast, O₂^{•-} almost did not contribute to the PEC bacteria inactivation when N₂ was aerated in the solution to remove O₂ to eliminate O₂^{•-}. Thus, produced h⁺ at the valence band was predominantly responsible for the PEC inactivation. This phenomenon is mainly due to the fact that the charge combination in a PEC process is effectively suppressed to enable a prolonged lifetime of h⁺ for instantaneous inactivation via direct h⁺ reactions [33]. Comparatively, the major RSs are completely different in the PC system. That is, h⁺ is mainly consumed to generate other RSs, especially

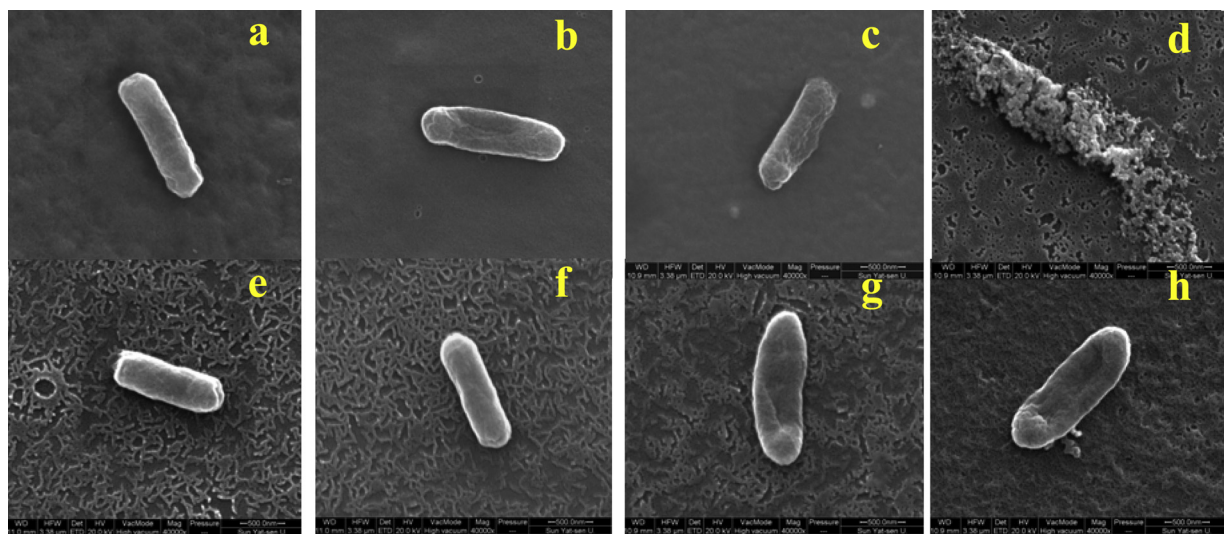


Fig. 4. SEM images of PEC inactivation of *E. coli* K-12 [(a) 0, (b) 70, (c) 180, and (d) 370 s] and *E. coli* BW25113 [(e) 0, (f) 70, (g) 180, and (h) 370 s].

•OH rather than directly attack the target bacteria in the PC system [7,9].

3.3. Bacterial destruction by PEC

To better understand the destruction of *E. coli* K-12 and its mutant *E. coli* BW25113, SEM was employed to examine the cell morphological changes during PEC treatment (Fig. 4). Both strains exhibited intact cell structure and well-preserved rod shape prior to the treatment (Fig. 4a and e). However, *E. coli* K-12 with abnormal and depressed shapes were observed after 70 s (Fig. 4b), indicating that the cell wall was damaged and cell permeability increased, which subsequently resulted in a leakage of the intracellular contents. Prolonging the reaction time to 180 and 370 s (Fig. 4c and d) resulted in progressive PEC action that increased cell permeability, more severe damages and the overall cell wall decomposition. Compared with *E. coli* K-12, the cell morphological changes and damages of *E. coli* BW25113 during PEC treatment were not evident at a corresponding resident time (Fig. 4e–h). For a 70 s treatment, *E. coli* BW25113 cell still exhibited well-preserved rod shape and intact membrane surface, even for the prolonged treatment times of 180 and 370 s, no severe damage of the cell wall can be observed, although obvious distortion-shaped cells were evidenced. The results further validated that the *E. coli* BW25113 showed higher resistance to PEC treatment than *E. coli* K-12.

The different susceptibilities and responses of the two strains toward external stress, in this case the PC or PEC treatment, is probably due to the different genes possessed [30,38]. For the mutant *E. coli* BW25113, *lacZ*, *araBAD* and *rhaBAD* were knocked out from *E. coli* K-12 [38]. *LacZ* is known to encode the structural gene of β -galactosidase synthase, which is an intracellular enzyme that can cleave disaccharide lactose into glucose and galactose. *AraBAD* encodes the enzymes of L-arabinose catabolism to enable cell to absorb and catabolize pentose sugar L-arabinose naturally found in the polysaccharides of cell walls. *RhaBAD* encodes the enzymes for L-rhamnose catabolism. Thus, the absence of these three genes from *E. coli* K-12 will result in the variation of easily oxidized saccharide in a bacterial cell [34]. Once the cell wall and membrane barrier are compromised, the RSs could exert oxidative actions directly to all essential components of the bacteria in cytoplasm, thus leading to cell death and complete decomposition, as evidenced by SEM images shown in Fig. 4, indicating that *E. coli* BW25113 was more difficult to be decomposed than *E. coli* K-12. This condition explains

the significantly increased resistance of *E. coli* BW25113 mutant to PEC and PC processes than its *E. coli* K-12.

3.4. Electrolyte selection in PEC inactivation system

To evaluate the influence of chemical composition of electrolyte on PEC inactivation performance, various frequently used electrolytes such as NaNO_3 , NaClO_4 , Na_2SO_4 , and NaCl were investigated using identical concentrations of 0.2 M (Fig. 5). Both strains did not show evident differences in inactivation efficiencies when

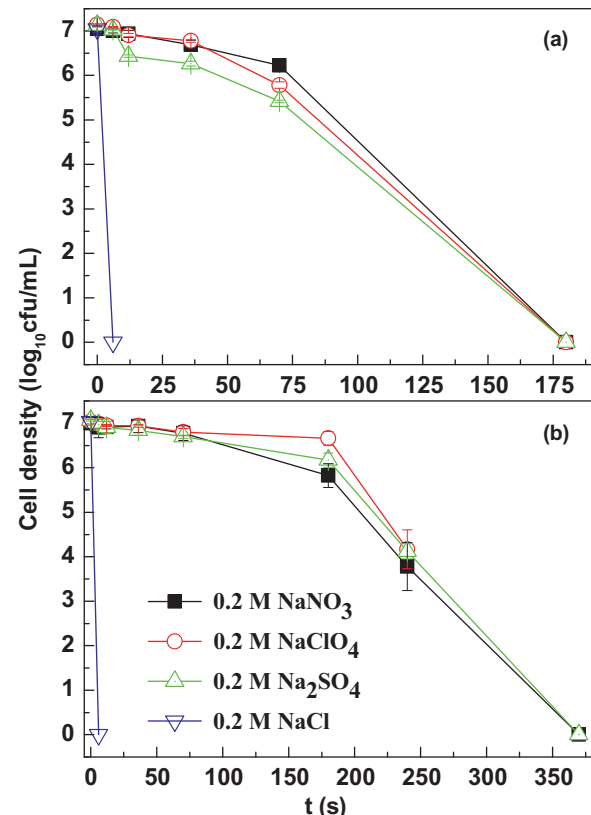


Fig. 5. Effects of different electrolytes on the PEC inactivation kinetics of *E. coli* K-12 (a) and *E. coli* BW25113 (b).

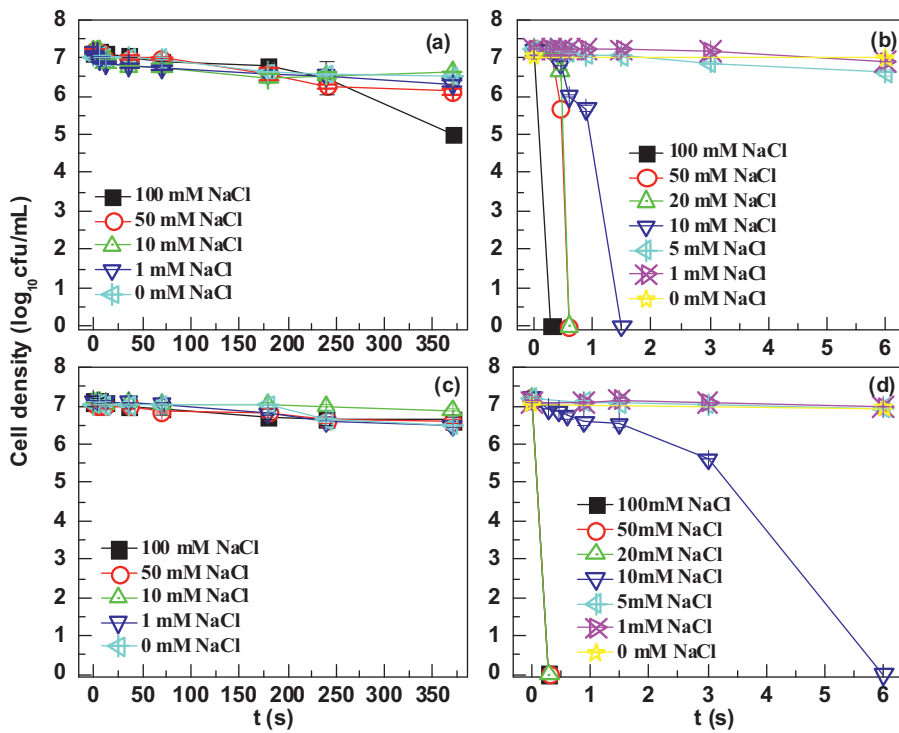


Fig. 6. Survived *E. coli* K-12 vs. PC (a) and PEC (b) inactivation time with different NaCl concentrations. Survived *E. coli* BW25113 vs. PC (c) and PEC (d) inactivation time with different NaCl concentrations.

NaNO_3 , NaClO_4 , and Na_2SO_4 were used as electrolyte, and the required time to completely inactivate *E. coli* K-12 and *E. coli* BW25113 were 180 and 370 s, respectively. This is because they only played a role for charge transport in solution during a PEC process rather than the active reactants involved in bactericide generation. Nevertheless, the presence of 0.2 M NaCl significantly increased the PEC inactivation efficiencies for both strains, and complete inactivation was achieved within 6 s. This is primarily due to that NaCl is well-known active electrolyte to accelerate the degradation of various organics during PEC process [39–42], although its application in bacterial inactivation is very limited [5]. Therefore, the enhancement mechanism of bacterial inactivation and inactivation kinetics response to different strains deserves a further investigation in the PEC system with NaCl as electrolyte compared with the PC system.

3.5. Effect of NaCl and NaBr concentration on PEC inactivation kinetics

The PC and PEC inactivation performances to both strains with addition of different concentrations of NaCl (PC-Cl/PEC-Cl) in 0.2 M NaNO_3 solution are illustrated in Fig. 6. For the PC-Cl system, the inactivation efficiencies of both strains were kept to almost zero within the investigated NaCl concentration ranging from 0 to 100 mM, except a 2.1-log inactivation was obtained at 100 mM NaCl for K-12 and 0.5-log for BW25113 within 370 s (Fig. 6a and c). That is, the addition of different NaCl concentrations hardly influenced the inactivation efficiencies of both bacterial strains. Notably, the lowest PC-Cl inactivation efficiencies of both strains were observed with addition of 10 mM NaCl, which could almost completely inhibit PC inactivation of bacteria. This phenomenon may be attributed to the reduction in oxidation efficiencies caused by Cl^- by scavenging RSs to form lower oxidation power species $\text{Cl}\bullet$ ($E^0[\text{Cl}\bullet/\text{Cl}^-] = +2.41 \text{ V}$) [43] than •OH (2.72 V) or by blocking the photoactive sites of TiO_2 nanotubular photoanode surface. Consequently, PC inactivation was significantly decreased [5,44]. Similar

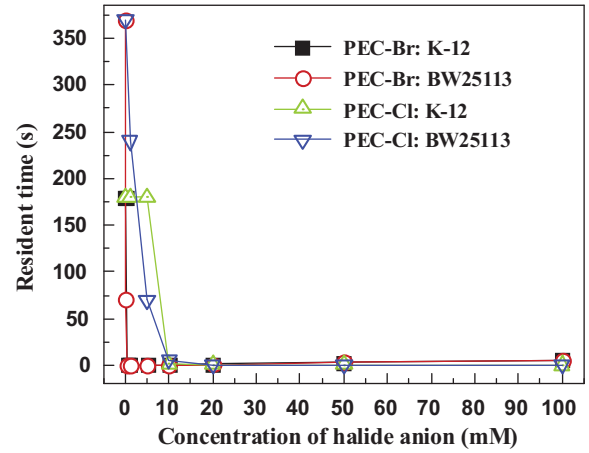


Fig. 7. Resident times of complete PEC inactivation of *E. coli* K-12 and *E. coli* BW25113 with different NaCl and NaBr concentrations.

results were also reported in PC-Cl decolorization of methylene blue [45,46]. When the NaCl concentration is increased up to 100 mM, the slight inactivation efficiency enhancement for both strains could be attributed to the excess Cl^- reacted with $\text{Cl}\bullet$ to form long-lived, stable, and reactive radicals $\text{Cl}_2\bullet^-$ toward organics and bacteria [44]. Furthermore, *E. coli* BW25113 mutant also shows higher resistance to PC-Cl than *E. coli* K-12, which may also be due to similar reasons as the aforementioned gene knockout.

Comparatively, NaCl addition could significantly increase PEC inactivation efficiencies of both strains. For *E. coli* K-12, the PEC-Cl inactivation efficiency remained zero within 6 s, and a prolonged treatment time of 180 s resulted in a 100% inactivation when 0 to 5 mM NaCl were added (Fig. 7). When the added NaCl was higher than 10 mM, the inactivation efficiency of *E. coli* K-12 dramatically increased and complete inactivation of $1.1 \times 10^7 \text{ CFU mL}^{-1}$ bacterial cells was achieved within 1.5 s (Figs. 6b and 7). When NaCl

Table 1Kinetic parameters of PEC inactivation *E. coli* K-12 and *E. coli* BW25113 with different NaCl and NaBr concentrations.

Parameters	Reagents	Strains	C (mM)								
			0	0.1	0.5	1	5	10	20	50	100
S_L (s)	NaCl	<i>E. coli</i> K-12	59.15	–	–	168.62	166.04	0.78	0.44	0.41	–
			0.13	–	–	0.23	0.22	21.76	105.06	87.69	–
		<i>E. coli</i> BW25113	141.99	–	–	24.52	12.16	2.36	–	–	–
			0.07	–	–	0.05	0.27	4.31	–	–	–
S_L (s)	NaBr	<i>E. coli</i> K-12	59.15	54.78	0.42	–	0.24	0.44	0.86	1.26	2.88
			0.13	0.13	35.06	–	49.61	105.49	25.31	9.39	5.12
		<i>E. coli</i> BW25113	141.99	25.78	–	–	–	0.30	0.60	1.32	3.09
			0.07	0.35	–	–	–	107.27	55.38	9.85	5.63

 S_L , shoulder length; k_{\max} , the slope of inactivation *E. coli* in the second period.

concentrations were increased to 20, 50, and 100 mM, the PEC-Cl inactivation efficiencies increased gradually, and the time for complete inactivation of *E. coli* K-12 further shortened from 0.6 to 0.3 s. However, for *E. coli* BW25113, the inactivation efficiencies also exhibited a monodirectional increase tendency similar to *E. coli* K-12. The required time to completely inactivate *E. coli* BW25113 was reduced from over 370 to 6 s when NaCl concentrations were increased from 0 to 10 mM (Figs. 6d and 7). When NaCl concentration was above 20 mM, 0.3 s was sufficient to kill all cells. Accordingly, it can be concluded that PEC-Cl showed higher inactivation efficiency toward *E. coli* BW25113 than *E. coli* K-12 when NaCl concentration was above 20 mM. This finding indicates that *E. coli* BW25113 is more susceptible to PEC-Cl than *E. coli* K-12 under high NaCl concentration. This may be attributed to the change of certain components in the mutant, which is susceptible to RSs produced in PEC-Cl with the addition of high NaCl concentration.

The inactivation kinetic curves of bacteria can generally be divided into three regions according to the modified Hom model [47]: (i) an initial smooth decay period known as “shoulder” at the beginning period of the reaction. At this stage, bacterial population is almost consistently stable. Various RSs begin to attack the bacteria, but they are insufficient to cause remarkable bacterial death; (ii) the second period is the main part of inactivation called the log-linear inactivation region caused by the fast bacterial inactivation as a consequence of the accumulative bacterial damages, leading to instant death; (iii) the last period is the “tail” region in which a deceleration occurs for the competition between the bacteria and organic by-products produced from bacterial decomposition [47]. In this work, the PEC-Cl inactivation kinetic parameters of both strains were also fitted using a modified Hom model via Microsoft Excel tool called GlnaFIT (Table 1). It should be noted that no “tail region” was obtained from all recorded inactivation curves as shown in Fig. 6. That is, no deceleration step was found for PEC-Cl inactivation, indicating an efficient inactivation process for both strains. Other two kinetic parameters, namely, S_L (shoulder length) and k_{\max} (the slope of the inactivation *E. coli* in the second period), were obtained by fitting the inactivation curves. Generally a shorter S_L and higher k_{\max} indicate higher inactivation efficiencies, which suggest the increase of RSs concentration. As shown in Table 1, with the increased NaCl from 1 to 5 mM, the fitted values of S_L and k_{\max} of *E. coli* K-12 remained at approximately 166.04 s and 0.22 CFU mL⁻¹ s⁻¹, respectively. However, when NaCl increased from 10 to 50 mM, S_L decreased remarkably from 0.78 to 0.4 s along with an increase in k_{\max} from 21.76 to 87.69 CFU mL⁻¹ s⁻¹, indicating a remarkable increase of RSs concentration. When NaCl was above 100 mM, S_L was negative, suggesting a rapid inactivation that can instantly kill all bacteria within 0.3 s without any inhibition period because of higher concentrations of photocatalytically generated RSs. For *E. coli* BW25113, S_L decreased gradually from 24.52 to 12.16 and further to 2.36 s along with an increase in k_{\max} from 0.05 to 0.27 and then to 4.31 CFU mL⁻¹ s⁻¹ as NaCl increased from 1 to 5 and then to 10 mM. Further increase of NaCl above

20 mM resulted in the negative value of S_L because of the instant inactivation of all bacteria cells of *E. coli* BW25113.

This study extends the investigation to include Br⁻ on the PC (PC-Br) and PEC (PEC-Br) inactivation (Fig. 8). The PC-Br and PEC-Br inactivation efficiencies were found to be more effective than those of PC-Cl and PEC-Cl for both strains. For the PC-Br process, although complete inactivation was not achieved within 370 s, ca. 2, 1.5, 5 and 6-log reductions in the *E. coli* K-12 cell population were observed in presence of 1, 10, 50, and 100 mM NaBr, respectively (Fig. 8a). Comparatively, only 0.9, 1.3, 4 and 5-log inactivation were obtained for *E. coli* BW25113 (Fig. 8c) with the corresponding NaBr concentrations. These results indicate that PC-Br inactivation of *E. coli* K-12 was more efficient than that of *E. coli* BW25113 under the same conditions. Comparatively, the required time to completely inactivate both strains was much shorter, and the “tail” region was also not observed for PEC-Br treatment (Fig. 8b and d). Furthermore, PEC-Br inactivation efficiencies of the two strains initially increased to a peak value when 0 to 1 mM of NaBr were added and then decreased with further increase of NaBr concentration. The time required to completely inactivate both strains in the PEC-Br system with different NaBr concentrations are shown in Fig. 7, and the calculated kinetic parameters are also presented in Table 1. Evidently, the time required for complete inactivation, S_L , and k_{\max} of *E. coli* K-12 in the presence of 0.1 mM NaBr were close to the case without NaBr. With the increased NaBr from 0.1 to 1 mM, PEC-Br inactivation efficiencies greatly increased, and the time required for complete inactivation sharply decreased from 180 to 0.30 s. Comparatively, 1.47 s was needed to completely inactivate the same strain under identical conditions except TiO₂ nanoparticle thin film photoanode [5]. This phenomenon suggests that the TiO₂ nanotubular photoanode could remarkably enhance the separation of photo-generated electron–hole pairs and lead to higher bactericidal activity. As the NaBr concentration increased from 0.1 to 0.5 mM, the fitted values of S_L of *E. coli* K-12 decreased from 54.78 to 0.42 s along with the increased k_{\max} from 0.13 to 35.06 CFU mL⁻¹ s⁻¹. Markedly, the negative value of S_L was obtained at 1 mM NaBr, suggesting that the complete inactivation could be instantly achieved. This phenomenon could be due to the fact that the highest RSs concentrations could be achieved under such experimental conditions. Further increased NaBr from 5 to 100 mM decreased the inactivation efficiency, and prolonged the resident time for the complete inactivation. S_L increased from 0.24 to 2.88 s along with the decrease in k_{\max} from 49.61 to 5.12 CFU mL⁻¹ s⁻¹. Evidently, the highest k_{\max} value of 105.49 CFU mL⁻¹ s⁻¹ was achieved at 10 mM NaBr. Although the required resident time for the complete inactivation was found to be identical to 5 and 10 mM NaBr, S_L for 5 mM NaBr was shorter than that of 10 mM NaBr. Similarly, PEC-Br inactivation efficiencies of *E. coli* BW25113 were higher than those cases without NaBr. The required time to completely inactivate the BW25113 was reduced from 370 s (without NaBr) to 70 s (in the presence of 0.1 mM NaBr). With increasing NaBr from 0.5 to

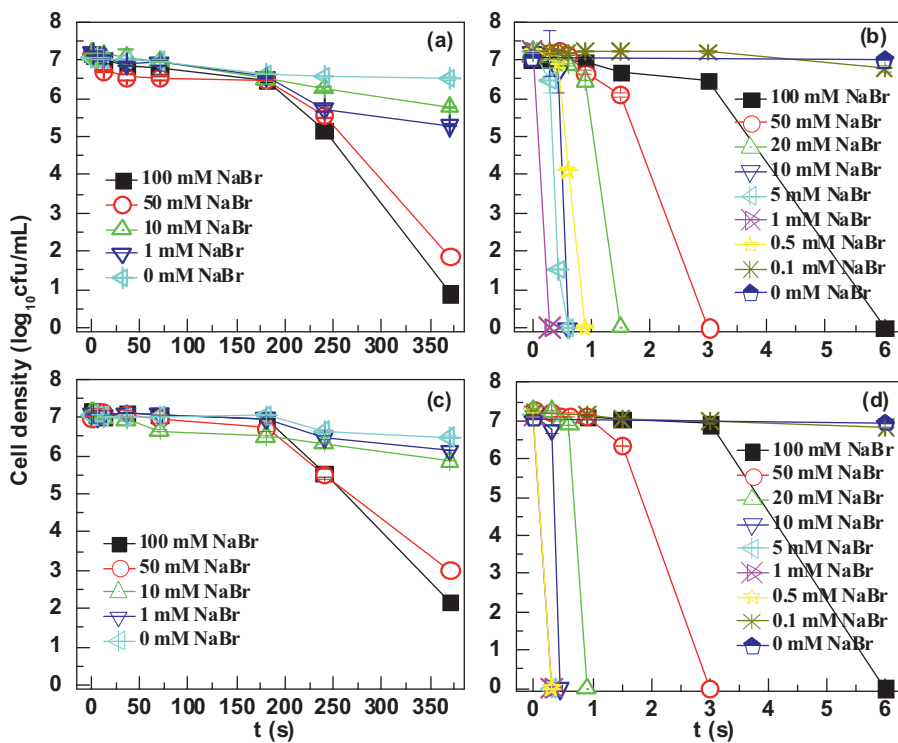


Fig. 8. Survived *E. coli* K-12 vs. PC (a) and PEC (b) inactivation time with different NaBr concentrations. Survived *E. coli* BW25113 vs. PC (c) and PEC (d) inactivation time with different NaBr concentrations.

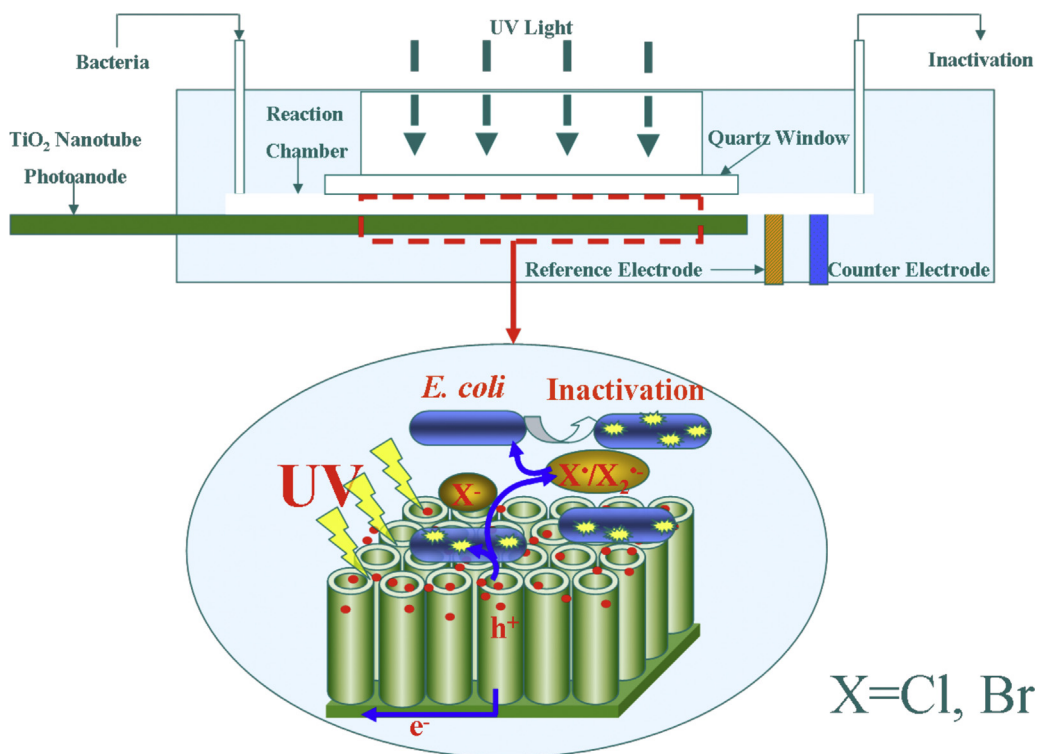
5 mM, all *E. coli* BW25113 cells were inactivated within 0.30 s, and S_L was negative, suggesting rapid inactivation of this strain. When NaBr concentration was greater than 10 mM, a decreased inactivation performance was observed, and the required durations for the complete inactivation were prolonged to 0.45 and 6.00 s with 10 and 100 mM NaBr, respectively. Simultaneously, S_L increased gradually from 0.30 to 3.09 s, and k_{max} decreased from 107.27 to 5.63 CFU mL⁻¹ s⁻¹.

Based on the results, although *E. coli* BW25113 exhibited higher resistance toward PEC treatment without halide ions, the presence of NaCl or NaBr could increase inactivation efficiency toward both strains. Under identical experimental conditions, however, no noticeable enhancement was observed for PC inactivation, especially for PC-Cl. This is mainly due to the rapid charge recombination in a PC process, leading to a decreased concentration of RSs, especially Cl[•] in the PC-Cl system. Consequently, the PC inactivation efficiency was significantly decreased. The change in inactivation efficiencies is closely correlated to the added amount of halide ions. Inactivation efficiencies at lower NaBr concentrations were higher than those under identical NaCl concentrations. Complete inactivation of both strains could be achieved by PEC within 0.30 s in presence of 1 mM NaBr or 100 mM NaCl, but the reverse results were observed at high concentrations of both halides. On the contrary, the incomplete inactivation of both strains was observed for PC within 370 s in presence of 0 to 100 mM NaCl or NaBr although the two strains exhibited different responses. This phenomenon may be attributed to the change of certain components in the mutant bacterial cell, which are susceptible to high concentration halogen radicals and dihalide radical anions.

A fundamental understanding of the underlying principles of the inactivation mechanism of different bacteria is critically important. **Scheme 1** shows the PEC bactericidal mechanism assisted by halide ions using nanotubular TiO₂ photoanode in a thin-layer reactor. In this system, the results strongly suggest that besides photo-generated h⁺, several other new RSs are also responsible

for the bactericidal enhancement in PEC-X (X: Br or Cl) system and a synergistic effect was obviously found between the PEC and addition of halide ions. As known, there was no other oxidation states of halogens existed [5]. Therefore, in the PEC-X system, Cl⁻ and Br⁻ could react with h⁺ to form halogen radicals (h⁺ + X⁻ → X[•]) like chloride radicals (Cl[•]) ($E^0[Cl^{\bullet}/Cl^-] = +2.41$ V) and bromide radicals (Br[•]) ($E^0[Br^{\bullet}/Br^-] = +1.94$ V) [43,48], which have highly reactive nature, strong oxidation power, and hence superior bactericidal performance. In addition, in the PEC process, the e⁻ can be timely removed by the application of an external bias. Thus, the effective separation of photo-generated electron–hole pairs could increase the concentration of photo-generated h⁺, leading to a significantly increased X[•] concentration in the PEC-X system. Meanwhile, the excess halide ions can be readily and rapidly combined with X[•] to produce stable and long-lived dihalide radical anions (Cl₂^{•-} and Br₂^{•-}) (Cl[•] + Cl⁻ ↔ Cl₂^{•-}, $K = 1.4 \times 10^5$ M⁻¹; Br[•] + Br⁻ ↔ Br₂^{•-}, $K = 3.9 \times 10^5$ M⁻¹) [49]. The formed X₂^{•-} can act as a bactericide to inactivate bacteria and their debris due to its high stability and powerful oxidative ability ($E^0[Cl_2^{\bullet-}/2Cl^-] = +2.11$ V, $E^0[Br_2^{\bullet-}/2Br^-] = +1.66$ V) [49] (**Scheme 1**). Eventually, the inactivation efficiencies were substantially enhanced [5,44]. Therefore, in addition to •OH and h⁺, X[•] and X₂^{•-} also played very important role in the long-range bactericidal effect in PEC-X system.

Although Cl[•] possesses a stronger oxidation power than Br[•], the observed inactivation efficiencies in the presence of Cl⁻ were nevertheless lower than that of Br⁻ under the same concentration. This can be interpreted as the rate of Cl[•] formation was much slower than Br[•] even with higher Cl⁻ concentration. Moreover, the reaction equilibrium constant for the formation of Br₂^{•-} ($K = 3.9 \times 10^5$ M⁻¹) is higher than that of Cl₂^{•-} ($K = 1.4 \times 10^5$ M⁻¹) [49], suggesting that the formation of Br₂^{•-} is more favorable than that of Cl₂^{•-}. However, an increase in Br⁻ above 1 mM could result in a slight decrease in bactericidal efficiency in PEC-Br process. This finding is probably due to the fact that a higher Br₂^{•-} concentration could affect the absorption of photons with a wavelength of 360 nm to reduce



Scheme 1. The PEC bactericidal mechanism assisted by halide ions using TiO_2 nanotubular photoanode in a thin-layer reactor.

photo-generated electron–holes pairs, and thus hindering the further formation of RSs [50]. Therefore, photo-generated holes and new formed RSs both have important attribution to the bactericidal performance in PEC-X system.

4. Conclusions

For both ancestor *E. coli* K-12 and its mutant *E. coli* BW25113, the obtained PEC bactericidal efficiencies were higher than those of PC because of more effective utilization of photo-generated holes. The nanotubular-structured TiO_2 photoanode was found to be beneficial in enhancing PEC inactivation efficiencies and facilitating charge transfer process, resulting in an increased inactivation efficiency of both strains. Mutant *E. coli* BW25113 exhibited a significantly increased resistance to PC and PEC processes as a different genotype compared with *E. coli* K-12. Photocatalytically generated holes were found to be predominantly responsible for the PEC disinfection because of the direct contact of the cell body to the surface of the TiO_2 nanotubular photoanode in the thin layer reactor. No obvious differences in inactivation efficiencies were found for both strains with different electrolytes of NaNO_3 , NaClO_4 , and Na_2SO_4 in the PEC process. However, the addition of NaCl or NaBr had a remarkable enhancement effect on the inactivation efficiencies of the two strains in PEC-X process. The shortest required treatment time for complete inactivation of two strains was obtained within 0.30 s with 1 mM NaBr or 100 mM NaCl , whereas no significant beneficial effect was observed for the PC process. The production of X^\bullet and $\text{X}_2^\bullet-$ was considered as the main factor responsible for the enhanced inactivation efficiencies in presence of halide ions in PEC-X processes.

Acknowledgements

This is contribution No. IS-1755 from GIGCAS. This work was supported by NSFC (21077104) and NSFC-Guangdong Joint Funds (No. U1201234), Guangzhou Institute of Geochemistry, CAS

(GIGCX-10-01), and partially supported by a General Research Fund (GRF 476811) to P.K. Wong.

References

- [1] B. Barbeau, L. Boulos, R. Desjardins, J. Coallier, M. Prevost, *Water Res.* 33 (1999) 2941–2948.
- [2] N.K. Hunt, B.J. Marinas, *Water Res.* 31 (1997) 1355–1362.
- [3] K.M. Ruffell, J.L. Rennecker, B.J. Marinas, *Water Res.* 34 (2000) 868–876.
- [4] J.A. Pals, J.K. Ang, E.D. Wagner, M.J. Plewa, *Environ. Sci. Technol.* 45 (2011) 5791–5797.
- [5] G.Y. Li, X.L. Liu, H.M. Zhang, T.C. An, S.Q. Zhang, A.R. Carroll, H.J. Zhao, *J. Catal.* 277 (2011) 88–94.
- [6] T. Matsunaga, R. Tomoda, T. Nakajima, H. Wake, *FEMS Microbiol. Lett.* 29 (1985) 211–214.
- [7] A. Markowska-Szczupak, K. Ulfig, A.W. Morawski, *Catal. Today* 169 (2011) 249–257.
- [8] D.M. Blake, P.C. Maness, Z. Huang, E.J. Wolfrum, J. Huang, W.A. Jacoby, *Sep. Purif. Method* 28 (1999) 1–50.
- [9] H.A. Foster, I.B. Ditta, S. Varghese, A. Steele, *Appl. Microbiol. Biotechnol.* 90 (2011) 1847–1868.
- [10] R.J. Watts, S.H. Kong, M.P. Orr, G.C. Miller, B.E. Henry, *Water Res.* 29 (1995) 95–100.
- [11] Y.W. Cheng, R.C.Y. Chan, P.K. Wong, *Water Res.* 41 (2007) 842–852.
- [12] A. Pal, S.O. Pehkonen, L.E. Yu, M.B. Ray, *J. Photochem. Photobiol. A: Chem.* 186 (2007) 335–341.
- [13] Y.M. Chen, A.H. Lu, Y. Li, L.S. Zhang, H.Y. Yip, H.J. Zhao, T.C. An, P.K. Wong, *Environ. Sci. Technol.* 45 (2011) 5689–5695.
- [14] O.K. Dalrymple, E. Stefanakos, M.A. Trotz, D.Y. Goswami, *Appl. Catal. B: Environ.* 98 (2010) 27–38.
- [15] Z.X. Lu, L. Zhou, Z.L. Zhang, W.L. Shi, Z.X. Xie, H.Y. Xie, D.W. Pang, P. Shen, *Langmuir* 19 (2003) 8765–8768.
- [16] M. Cho, H. Chung, W. Choi, J. Yoon, *Water Res.* 38 (2004) 1069–1077.
- [17] N. Baram, D. Starovetsky, J. Starovetsky, M. Epshtein, R. Armon, Y. Ein-Eli, *Appl. Catal. B: Environ.* 101 (2011) 212–219.
- [18] M. Cho, E.L. Cates, J.H. Kim, *Water Res.* 45 (2011) 2104–2110.
- [19] P.A. Christensen, T.P. Curtis, T.A. Egerton, S.A.M. Kosa, J.R. Tinlin, *Appl. Catal. B: Environ.* 41 (2003) 371–386.
- [20] C. Pablos, R. van Grieken, J. Marugan, B. Moreno, *Catal. Today* 161 (2011) 133–139.
- [21] R. van Grieken, J. Marugan, C. Sordo, P. Martinez, C. Pablos, *Appl. Catal. B: Environ.* 93 (2009) 112–118.
- [22] S.C. Hayden, N.K. Allam, M.A. El-Sayed, *J. Am. Chem. Soc.* 132 (2010) 14406–14408.

- [23] N. Baram, D. Starosvetsky, J. Starosvetsky, M. Epshtein, R. Armon, Y. Ein-Eli, *Electrochim. Acta* 54 (2009) 3381–3386.
- [24] P.S.M. Dunlop, T.A. McMurray, J.W.J. Hamilton, J.A. Byrne, *J. Photochem. Photobiol. A: Chem.* 196 (2008) 113–119.
- [25] C.A. Grimes, K. Shankar, J.I. Basham, N.K. Allam, O.K. Varghese, G.K. Mor, X.J. Feng, M. Paulose, J.A. Seabold, K.S. Choi, *J. Phys. Chem. C* 113 (2009) 6327–6359.
- [26] Y. Ein-Eli, N. Baram, D. Starosvetsky, J. Starosvetsky, M. Epshtein, R. Armon, *Appl. Catal. B: Environ.* 101 (2011) 212–219.
- [27] P. Roy, S. Berger, P. Schmuki, *Angew. Chem. Int. Ed.* 50 (2011) 2904–2939.
- [28] G.L. Yan, J. Chen, Z.Z. Hua, *J. Photochem. Photobiol. A: Chem.* 207 (2009) 153–159.
- [29] O.K. Dalrymple, W. Isaacs, E. Stefanakos, M.A. Trotz, D.Y. Goswami, *J. Photochem. Photobiol. A: Chem.* 221 (2011) 64–70.
- [30] M.H. Gao, T.C. An, G.Y. Li, X. Nie, H.Y. Yip, H. Zhao, P.K. Wong, *Water Res.* 46 (2012) 3951–3957.
- [31] X. Nie, J.Y. Chen, G.Y. Li, H.X. Shi, H.J. Zhao, P.K. Wong, T.C. An, *J. Chem. Technol. Biotechnol.* 88 (2013) 1488–1497.
- [32] K. Shankar, J.I. Basham, N.K. Allam, O.K. Varghese, G.K. Mor, X. Feng, M. Paulose, J.A. Seabold, K.-S. Choi, C.A. Grimes, *J. Phys. Chem. C* 113 (2009) 6327–6359.
- [33] G.Y. Li, X.L. Liu, H.M. Zhang, P.K. Wong, T.C. An, H.J. Zhao, *Appl. Catal. B: Environ.* 140/141 (2013) 225–232.
- [34] X. Quan, S. Yang, X. Ruan, H. Zhao, *Environ. Sci. Technol.* 39 (2005) 3770–3775.
- [35] D.L. Jiang, S.Q. Zhang, H.J. Zhao, *Environ. Sci. Technol.* 41 (2007) 303–308.
- [36] D.L. Jiang, H.J. Zhao, S.Q. Zhang, R. John, *J. Phys. Chem. B* 107 (2003) 12774–12780.
- [37] Y. Hou, X.Y. Li, Q.D. Zhao, X. Quan, G.H. Chen, *Adv. Funct. Mater.* 20 (2010) 2165–2174.
- [38] T. Baba, T. Ara, M. Hasegawa, Y. Takai, Y. Okumura, M. Baba, K.A. Datsenko, M. Tomita, B.L. Wanner, H. Mori, *Mol. Syst. Biol.* 2 (2006).
- [39] T.C. An, W.B. Zhang, X.M. Xiao, G.Y. Sheng, J.M. Fu, X.H. Zhu, *J. Photochem. Photobiol. A: Chem.* 161 (2004) 233–242.
- [40] T.C. An, W.B. Zhang, G.Y. Li, J.M. Fu, G.Y. Sheng, *Chinese Chem. Lett.* 15 (2004) 455–458.
- [41] G.Y. Li, T.C. An, X.P. Nie, G.Y. Sheng, X.Y. Zeng, J.M. Fu, Z. Lin, E.Y. Zeng, *Environ. Toxicol. Chem.* 26 (2007) 416–423.
- [42] G.Y. Li, T.C. An, J.X. Chen, G.Y. Sheng, J.M. Fu, F.Z. Chen, S.Q. Zhang, H.J. Zhao, *J. Hazard. Mater.* 138 (2006) 392–400.
- [43] J.E. Rogers, B. Abraham, A. Rostkowski, L.A. Kelly, *Photochem. Photobiol.* 74 (2001) 521–531.
- [44] A.G. Rincon, C. Pulgarin, *Appl. Catal. B: Environ.* 51 (2004) 283–302.
- [45] J. Marugan, R. van Grieken, C. Pablos, C. Sordo, *Water Res.* 44 (2010) 789–796.
- [46] T.C. An, Y. Xiong, G.Y. Li, C.H. Zha, X.H. Zhu, *J. Photochem. Photobiol. A: Chem.* 152 (2002) 155–165.
- [47] J. Marugan, R. van Grieken, C. Sordo, C. Cruz, *Appl. Catal. B: Environ.* 82 (2008) 27–36.
- [48] G. Merenyi, J. Lind, *J. Am. Chem. Soc.* 116 (1994) 7872–7876.
- [49] Y. Liu, A.S. Pimentel, Y. Antoku, B.J. Giles, J.R. Barker, *J. Phys. Chem. A* 106 (2002) 11075–11082.
- [50] M.M. Cheng, A. Bakac, *J. Am. Chem. Soc.* 130 (2008) 5600–5605.